JOURNAL OF INTERFERON & CYTOKINE RESEARCH
Volume 40, Number 8, 2020
Mary Ann Liebert, Inc.
DOI: 10.1089/jir.2020.0111

Novel Interleukin-6 Inducible Gene PDZ-Binding Kinase Promotes Tumor Growth of Multiple Myeloma Cells

Akinobu Ota,[1] Ichiro Hanamura,[2] Sivasundaram Karnan,[1] Shingo Inaguma,[3] Norio Takei,[4] Vu Quang Lam,[2] Shohei Mizuno,[2] Jo Kanasugi,[2] Md Wahiduzzaman,[1] Md Lutfur Rahman,[1] Toshinori Hyodo,[1] Hiroyuki Konishi,[1] Shinobu Tsuzuki,[1] Hiroshi Ikeda,[3] Akiyoshi Takami,[2] and Yoshitaka Hosokawa[1]

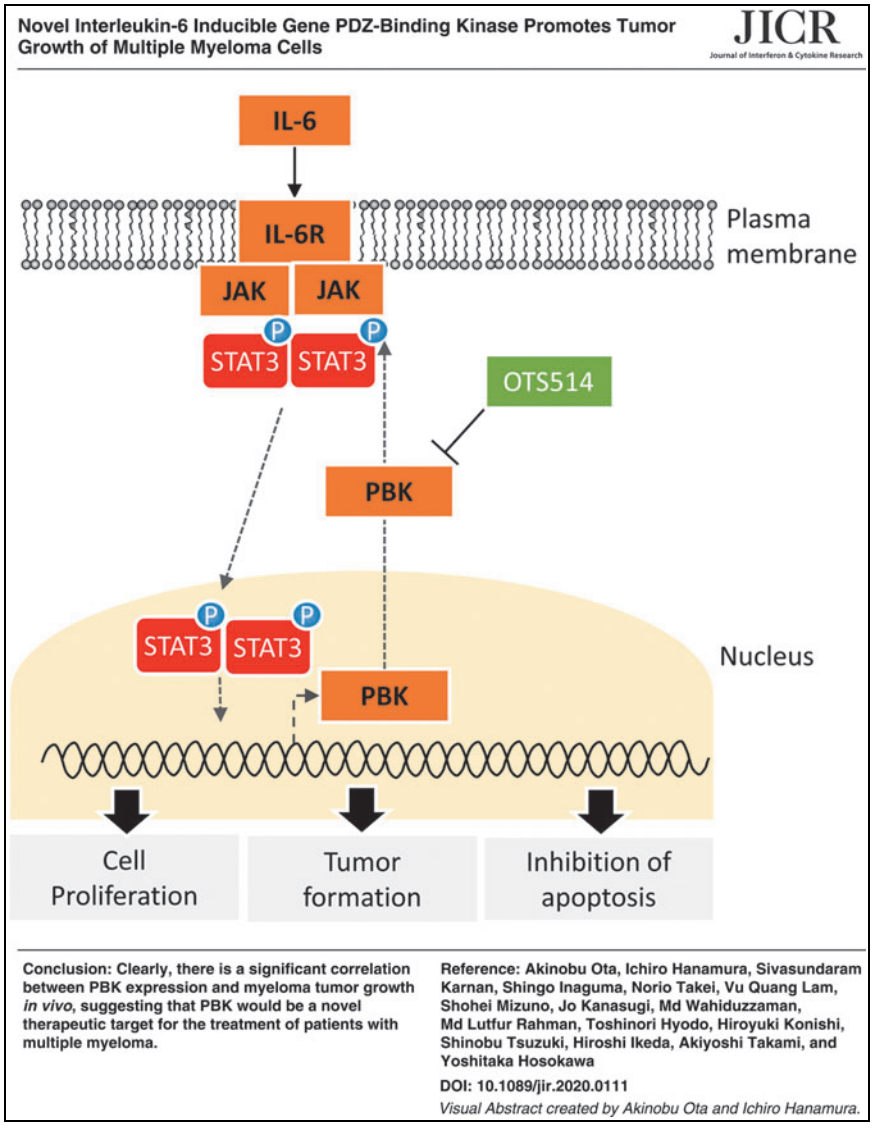

[1]Department of Biochemistry, Aichi Medical University School of Medicine, Nagakute, Japan.
[2]Division of Hematology, Department of Internal Medicine, Aichi Medical University School of Medicine, Nagakute, Japan.
[3]Department of Pathology, Aichi Medical University School of Medicine, Nagakute, Japan.
[4]Institute for Animal Experimentation, Faculty of Medicine, Hokkaido University, Sapporo, Japan.

Multiple myeloma (MM) remains an intractable hematological malignancy, despite recent advances in anti-MM drugs. Here, we show that role of PDZ binding kinase (PBK) in MM tumor growth. We identified that interleukin-6 (IL-6) readily increases PBK expression. Kaplan–Meier analysis showed that the MM patients with higher expression of PBK have a significant shorter survival time compared with those with moderate/lower expression of PBK. Knockout of *PBK* dramatically suppressed *in vivo* tumor growth in MM cells, while genome editing of *PBK* changing from asparagine to serine substitution (rs3779620) slightly suppresses the tumor formation. Mechanistically, loss of *PBK* increased the number of apoptotic cells with concomitant decrease in the phosphorylation level of Stat3 as well as caspase activities. A novel PBK inhibitor OTS514 significantly decreased KMS-11-derived tumor growth. These findings highlight the novel oncogenic role of PBK in tumor growth of myeloma, and it might be a novel therapeutic target for the treatment of patients with MM.

Keywords: multiple myeloma, interleukin-6, PBK, tumor growth, molecular-targeted therapy

Introduction

Multiple myeloma (MM) is a hematological malignancy caused by the abnormal expansion of bone marrow-derived plasma cells (Anderson and others 2011; Kumar and others 2017; Moreau and others 2017). MM primarily develops in the bone marrow microenvironment, where the bone marrow stromal cells support the survival and proliferation of MM cells by mediating expression of extracellular matrix proteins, cell surface molecules, and humoral factors, including interleukin-6 (IL-6) (Kawano and others 1998; Kishimoto 2010).

Recent accumulating evidence obtained using novel genomic approaches indicates the diversity of MM cells within individual patients and the complex pathophysiology of MM during its progression (Keats and others 2012; Kumar and others 2017). Although new classes of drugs have successfully prolonged the quality of life of MM patients, MM can subsequently progress into incurable bone marrow-independent diseases, such as extramedullary myeloma and plasma cell leukemia. Several prognostic factors and risk stratification that are based on cytogenetic abnormalities and biomarkers have been defined to predict the disease progression and prognosis (Boyd and others 2012; Mikhael and others 2013; Chng and others 2014). Therefore, novel therapeutics are required immediately to further improve the survival of patients with high-grade MMs.

PDZ-binding kinase (PBK), also known as T cell-originated protein kinase (TOPK), was initially identified as a mitotic kinase for mitogen-activated protein kinase (MAPK) and is involved in cytokinesis and spermatogenesis (Gaudet and others 2000; Matsumoto and others 2004; Fujibuchi and others 2005; Abe and others 2007; Park and others 2010). High expression of PBK is closely associated with patient survival and/or invasive phenotype of cancer, including hepatocellular carcinoma, gastric cancer, esophageal squamous cell carcinoma, prostate cancer, and oral cancer (Brown-Clay and others 2015; Chang and others 2016; Kwon and others 2016; Ohashi and others 2016, 2017; Yang and others 2017). It has been reported that PBK expression is controlled by E2F Transcription Factor 1 (E2F1), c-Myc, and forkhead box M1 (FoxM1) transcriptional factor, all of which are involved in cell proliferation (Hu and others 2013; Chen and others 2015; Yang and others 2017). Given the accumulating evidence showing the involvement of PBK in tumor progression, it would be of interest to investigate the role of PBK in the development of MM. However, the association of PBK expression with tumor proliferation of MM remains poorly understood.

In this study, we sought to examine the effect of PBK in the tumor growth of MM cells. To identify the genes related to myeloma cell growth, we performed comprehensive gene expression analysis using IL-6-independent human MM cell lines. Additionally, we obtained the gene expression data of a public cohort and verified the association of PBK expression with the overall survival (OS) of MM patients. To investigate the effect of PBK on the proliferation of MM cells, we generated human MM isogenic cell clones using genome editing technique. Furthermore, we proposed the molecular mechanism by which PBK plays a pivotal role in the survival of MM cells.

Materials and Methods

Reagents

RPMI-1640, penicillin–streptomycin solution, and trypsin-EDTA solution were purchased from Wako Pure Chemical Industries, Ltd. (Osaka, Japan). Thiazolyl Blue Tetrazolium Bromide (MTT) was purchased from Sigma-Aldrich (Tokyo, Japan). Mouse monoclonal anti-PBK antibody (B-10) was obtained from Santa Cruz Biotechnologies (Dallas, TX). Stat3 inhibitor SH-4-54 and a PBK inhibitor OTS514 were obtained from Selleck Chemicals, Inc. (Houston, TX).

Cell culture

Human MM cell lines, KMS-11, RPMI8226, KMM1, and FLAM-76, were obtained from the Japanese Collection of Research Bioresource Cell Bank. Human MM cell line, OCI-My5, was obtained from the Leibniz Institute DSMZ (Braunschweig, Germany). Human MM cell line, UTMC-2, was kindly provided by Dr. Shuji Ozaki (Tokushima Prefectural Central Hospital, Tokushima, Japan) (Ozaki and others 1994). IL-6-dependent MM cell line, ANBL-6, was kindly provided by Dr. Diane F. Jelinek (Mayo Clinic, Rochester, MN) (Jelinek and others 1993). Human MM cell lines, NCU-MM1 and AMU-MM1, were established at Nagoya City University Medical School and Aichi Medical University of Medicine, respectively (Iida and others 2000; Nagoshi and others 2012).

Gene expression analysis

IL-6-dependent cell lines, ANBL-6 and FLAM-76, were seeded in a six-well plate (5×10^5 cells/well), and the cells were incubated for 48 h in the absence of IL-6. Following

incubation for 48 h, the cells were treated with IL-6 (10 ng/mL) for 24 h. Total RNA was extracted by using NucleoSpin RNA with DNase treatment (TaKaRa Bio, Inc., Shiga, Japan). The experimental procedure for the complementary DNA (cDNA) microarray analysis was based on the manufacturer's protocol (Agilent Technologies, Santa Clara, CA), and has been described previously (Wahiduzzaman and others 2018). The raw microarray data have been submitted to the GEO database at NCBI (GSE115558). Gene set enrichment analysis (GSEA) was performed according to the instructions.

Quantitative reverse transcription–polymerase chain reaction analysis

Quantitative reverse transcription–polymerase chain reaction analysis was performed using SYBR Green I, as previously described (Takahashi and others 2013). Glyceraldehyde-3-phosphate dehydrogenase (*GAPDH*) was used as an internal control. The primers used in this study have been described in Supplementary Table S1.

Immunohistochemistry

Immunohistochemistry was performed to investigate the expression of PBK using anti-PBK antibody (B-10; Santa Cruz Biotechnologies). Human myeloma tissue slide was obtained from US Biomax, Inc. (Derwood, MD). Sequential sections of formalin-fixed, paraffin-embedded tissue samples were subjected to immunohistochemical staining and Hematoxylin/Eosin staining. Immunohistochemistry was performed using a Ventana BenchMark XT automated immunostainer with the iView (Roche Diagnostics, Basel, Switzerland) Detection Kit. Photographs were taken using a bright field microscope (BX-43; Olympus, Tokyo, Japan).

Western blot analysis

Western blot analysis was performed as described previously (Hossain and others 2015). The antibodies used in this study have been described in Supplementary Table S2. Immune complexes were detected using ImmunoStar LD (Wako Pure Chemical Industries, Ltd.) in conjunction with a LAS-4000 image analyzer (GE Healthcare, Tokyo, Japan). The full-length blots are included in Supplementary Fig. S1.

Luciferase reporter assay for PBK *promoter activity*

The 1216- (−1216 to +116) and 405- (−191 to +116) human *PBK* promoter region was amplified from genomic DNA of KMS-11 cells with KOD plus Neo polymerase (TOYOBO, Tokyo, Japan). The primer information has been indicated in Supplementary Table S1. The amplified DNA fragments were cloned into the pGL3 basic vector (Promega). Luciferase promoter activity assay was measured as described previously (Wahiduzzaman and others 2018).

PBK knockout using the clustered regularly interspaced short palindromic repeats-Cas9 system

Clustered regularly interspaced short palindromic repeats (CRISPR)-Cas9 system was used to disrupt the expression of *PBK* gene, as described elsewhere (Ota and others 2017). pSpCas9(BB)-2A-GFP (PX458) and lentiCRISPR v2 were gifts from Feng Zhang (Addgene plasmids No. 48138 for PX458 and No. 52961 for lentiCRISPR v2) (Ran and others 2013; Sanjana and others 2014). The single-guide RNA (sgRNA) sequence for *PBK* Exon 3 and Exon 5 were 5′-GAGGCCGGGATATTTATAGT and 5′-CGCTATCTGAG CAGCGCTCA, respectively. For lentivirus preparation, 293T cells (4×10^6 cells/dish) were seeded in a 10 cm dish 1 day before transfection. Lentiviral lentiCRISPR v2 containing PBK sgRNA, viral packaging vector psPAX2 (a gift from Didier Trono; Addgene plasmid No. 12260), and viral envelope vector pCMV-VSV-G (a gift from Bob Weinberg; Addgene plasmid No. 8454) (Stewart and others 2003) were diluted at a ratio of 4:3:2 in Opti-MEM medium (Thermo Fisher Scientific K.K., Tokyo, Japan).

Cell viability (MTT) assay

The MM cells were seeded in 96-well culture plates (1×10^4 cells/well) and were then incubated with culture medium. After incubation for 72 h, MTT assay was performed as described previously (Wahiduzzaman and others 2018). The absorbance at 545 nm was measured using a SpectraMAX M5 spectrophotometer (Molecular Devices, Sunnyvale, CA).

Soft agar colony formation assay

The soft agar colony formation assay was carried out as described previously (Wahiduzzaman and others 2018). The parental KMS-11 cells and KMS-11/*PBK*$^{-/-}$ cell clones (1×10^3 cells/well) were cast in 2 mL of top layer comprising 0.4% agarose (Bacto agar; BD Biosciences) and poured on top of a 2 mL bottom layer containing 0.6% agarose in six-well plates. After incubation for 14–17 days, the colonies were stained with MTT solution (5 mg/mL) in phosphate-buffered saline. Photographs were taken using a bright field microscope (IX-73; Olympus).

Annexin V assay

The Annexin V assay was carried out as described previously (Wahiduzzaman and others 2018). The MM cells were seeded in six-well culture plates (5×10^5 cells/well). Next, the cells were incubated with culture medium for 48 h, followed by incubation with Annexin V (Ax)-FITC and Propidium Iodide (PI; 10 μg/mL) at 25°C room temperature for 15 min. Finally, fluorescence intensities were determined by fluorescence-activated cell sorting (FACS) using a FACSCantoII (BD, Franklin Lakes, NJ).

Cell cycle analysis for sub-G1 population

The Cell cycle analysis for sub-G1 population was carried out as described previously (Wahiduzzaman and others 2018). The MM cells (5×10^5 cells/well) were seeded and incubated as described above. For FACS analysis, the cells were collected at 48 h after treatment and fixed in 70% ethanol overnight at −30°C. After fixation, the cells were treated with RNase A (100 μg/mL) and stained with PI (100 μg/mL). The percentages of cells in the sub-G1 phase were measured using FlowJo software (Tree Star, Inc., Ashland, OR).

Measurement of caspase-3/7 activity

The caspase -3/7 assay was performed using an Apo-ONE Homogeneous Caspase-3/7 Assay Kit (Promega KK, Tokyo, Japan) according to the manufacturer's instructions and as described previously (Wahiduzzaman and others 2018). Briefly, cells (1×10^4 cells/well) were seeded in a 96-well culture plate and were incubated for 24 h. Caspase-3/7 reagent (100 μL) containing Z-DEVD-R110 was added to each well. Fluorescence intensity (499 nm excitation and 521 nm emission) was measured using a SpectraMax M5 spectrophotometer (Molecular Devices).

Xenograft experiment

The use of animals for the study was approved by the Ethics Committee on the Institute of Animal Experiments of Aichi Medical University (No. 2018-67). All the experiment protocols for using mice in the study were followed according to relevant guidelines and regulation of animal care. Female FOX CHASE severely compromised immunodeficient (SCID) C.B-17/lcr-scid/scidJcl mice (6- to 8-week-old) were purchased from CLEA Japan, Inc. (Tokyo, Japan) and bred in accordance with the institution guidelines. Briefly, KMS-11 or 2×10^7 cells were injected subcutaneously into Scid mice. In mice injected with KMS-11 cells, when the tumor size had reached 500 mm^3, OTS514 (10 mg/kg, every 2 days) was intraperitoneally administered. Tumors and body weights were measured every 3 or 4 days. Tumor volume (mm^3) was calculated by using the modified ellipsoid formula 1/2 (length × $width^2$). At the same time, body weight was measured, and (1) when a weight increase of 10% or more and/or (2) when a tumor size increase of more than 2,000 mm^3 was observed as compared with noncancer-bearing mice of the same age, euthanasia was performed as a measure for reducing pain as early as possible. The central disruption (cervical dislocation) method was used as the method of euthanasia under anesthesia with isoflurane. After that, the cancer tissue was collected, total RNA and protein were extracted, and used for biochemical analysis. To minimize the number of animals used per experiment, we typically set the number of mice as 6 (up to 10), unless otherwise stated.

Statistical analyses

Statistical analyses were performed using SPSS software, version 23.0 (SPSS, Inc., Chicago, IL). Kaplan–Meier analysis was performed with EZR (Saitama Medical Center, Jichi Medical University, Saitama, Japan), which is a graphical user interface for R (Kanda 2013).

Results

IL-6 transcriptionally upregulates expression of PBK in human myeloma cells

IL-6 is well known to play a pivotal role in both survival and growth of MM cells (Kawano and others 1998). To investigate IL-6 inducible genes, which are associated with MM cell growth and related to prognosis of MM patients, we first examined the effect of IL-6 on gene expression changes in IL-6-dependent cell lines ANBL-6 and FLAM-76. We found that messenger RNA (mRNA) expression levels of several genes, including known IL-6-inducible gene *SPP1*, increased following 24 h of IL-6 treatment (Table 1). Among the genes, we found that the expression of PBK, a serine/threonine kinase, significantly increased in ANBL-6 cells in a time-dependent manner (Fig. 1A). We

Table 1. Upregulated Genes After Interleukin-6 Treatment in Interleukin-6-Dependent Multiple Myeloma Cell Lines

		FC[a]	
Gene symbol	*Description*	*FLAM-76*	*ANBL-6*
SOCS3	Suppressor of cytokine signaling 3	56.9	73.6
SPP1	Secreted phosphoprotein 1	13.7	33.6
CSF1R	Colony-stimulating factor 1 receptor	4	20.5
CLDN14	Claudin 14	6.2	13.3
ENST0000390465	T cell receptor alpha variable 38-2/delta variable 8	13.1	11.7
BCL6	B cell CLL/lymphoma 6	4.9	11.1
PTP4A3	Protein tyrosine phosphatase type IVA, member 3	8.6	8.9
ELF3	Ets domain transcription factor, epithelial-specific	2.7	8.4
SGK1	Serum/glucocorticoid-regulated kinase 1	4.8	6.6
HBB	Hemoglobin, beta	2.2	6.5
PARP9	Poly (ADP-ribose) polymerase family, member 9	9.6	6.2
DCC	Deleted in colorectal carcinoma	3.4	6.1
CYP21A2	Cytochrome P450, family 21, subfamily A, polypeptide 2	6.7	5.8
DSCC1	DNA replication and sister chromatid cohesion 1	3.1	5.7
CAPN5	Calpain 5	2.8	5.6
EGR1	Early growth response 1	6.8	5.3
PBK	**PDZ-binding kinase**	**3.7**	**5**
HBD	Hemoglobin, delta	3.2	5
EFEMP1	EGF-containing fibulin-like extracellular matrix protein 1	4.4	4.9

Bold values show the FC in gene expression of PBK at 24 h after IL-6 stimulation in IL-6-dependent MM cell lines.

[a]FC was calculated using cDNA microarray data as followed: dividing the Log_2 values of IL-6-treated cells (24 h) by the untreated cells. The raw microarray data have been submitted to the GEO database at NCBI (GSE115558).

cDNA, complementary DNA; FC, fold change; IL-6, interleukin-6.

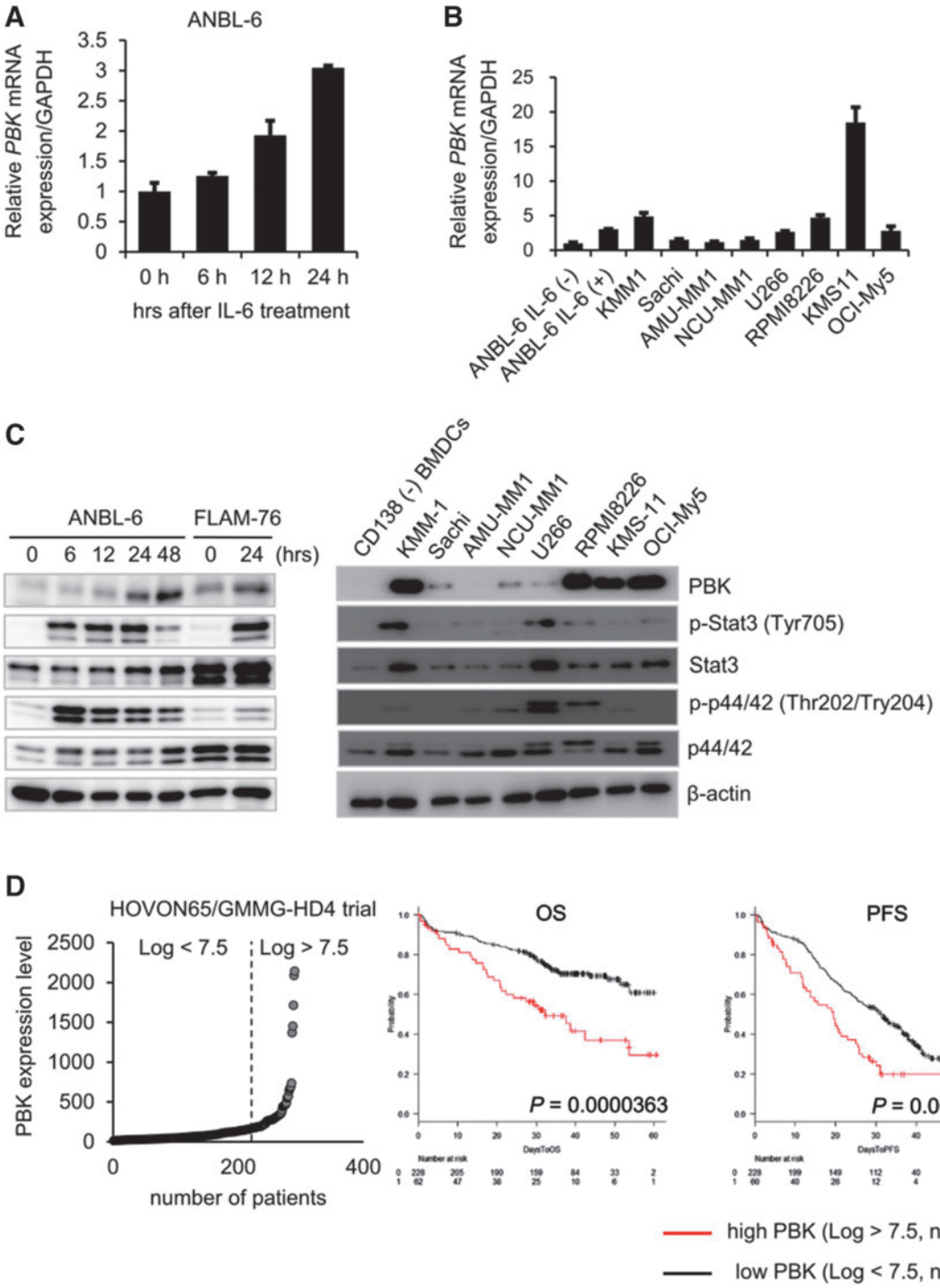

FIG. 1. Upregulation of PBK expression in MM cells. **(A)** IL-6-dependent MM cell line ANBL-6 cells were incubated with IL-6 (10 ng/mL) for indicated time points. mRNA expression of PBK in IL-6-treated cells are shown. **(B)** mRNA expression of PBK in IL-6-independent MM cell lines. **(C)** Protein expression of PBK in MM cells. *Left*, IL-6-dependent ANBL-6 and FLAM76 cells were incubated with IL-6 (10 ng/mL) at the indicated time points. *Right*, IL-6-independent MM cell lines and bone marrow-derived CD138-negative cells were incubated in a RPMI-1640 medium containing 10% FBS. **(D)** Kaplan–Meier analysis. Raw gene expression values of PBK in the MM patients are shown (*left*). Kaplan–Meier analysis was conducted to assess the value of PBK in overall (OS, *middle*) and progression-free (PFS, *right*) survival of patients with MM in the HOVON65/GMMG-HD4 cohort (GSE19784). **(E)** The $\log_2$ gene expression values of PBK in the cluster groups are shown (*left*). The 11 clusters were previously classified based on comprehensive gene expression analysis (Broyl and others 2010). MS, t(4;14); MF, t(14;16)/t(14;20); CD-1/2, t(11;14) and t(6;14); HY, a hyperdiploid cluster; PR, a cluster with proliferation-associated genes. Kaplan–Meier analysis was conducted to assess the value of PBK in OS (*middle*) and PFS (*right*) of patients with MM in the MS t(4;14) cluster in the cohort. **(F)** Immunohistochemistry for PBK expression in the patient-derived bone marrow tissues. The paraffin-embedded MM tissue section (T291b; US Biomax, Inc., Derwood, MD) was stained with anti-PBK mouse monoclonal antibody (*left panel*, sc-390399; 1:100 dilution). **(G)** PBK promoter activity was examined using a luciferase reporter assay. ANBL-6 cells were cotransfected with PBK-Luc vector (containing PBK promoter region −1216 to +116, −191 to +116 or no insert; firefly-luciferase) and the phRL-TK vector (internal control; Renilla-luciferase) followed by treatment with IL-6 (10 ng/mL) for 24 h ($n = 6$; $^*P < 0.05$). FBS, fetal bovine serum; IL-6, interleukin-6; MM, multiple myeloma; mRNA, messenger RNA; OS, overall survival; PBK, PDZ-binding kinase; PFS, progression-free survival.

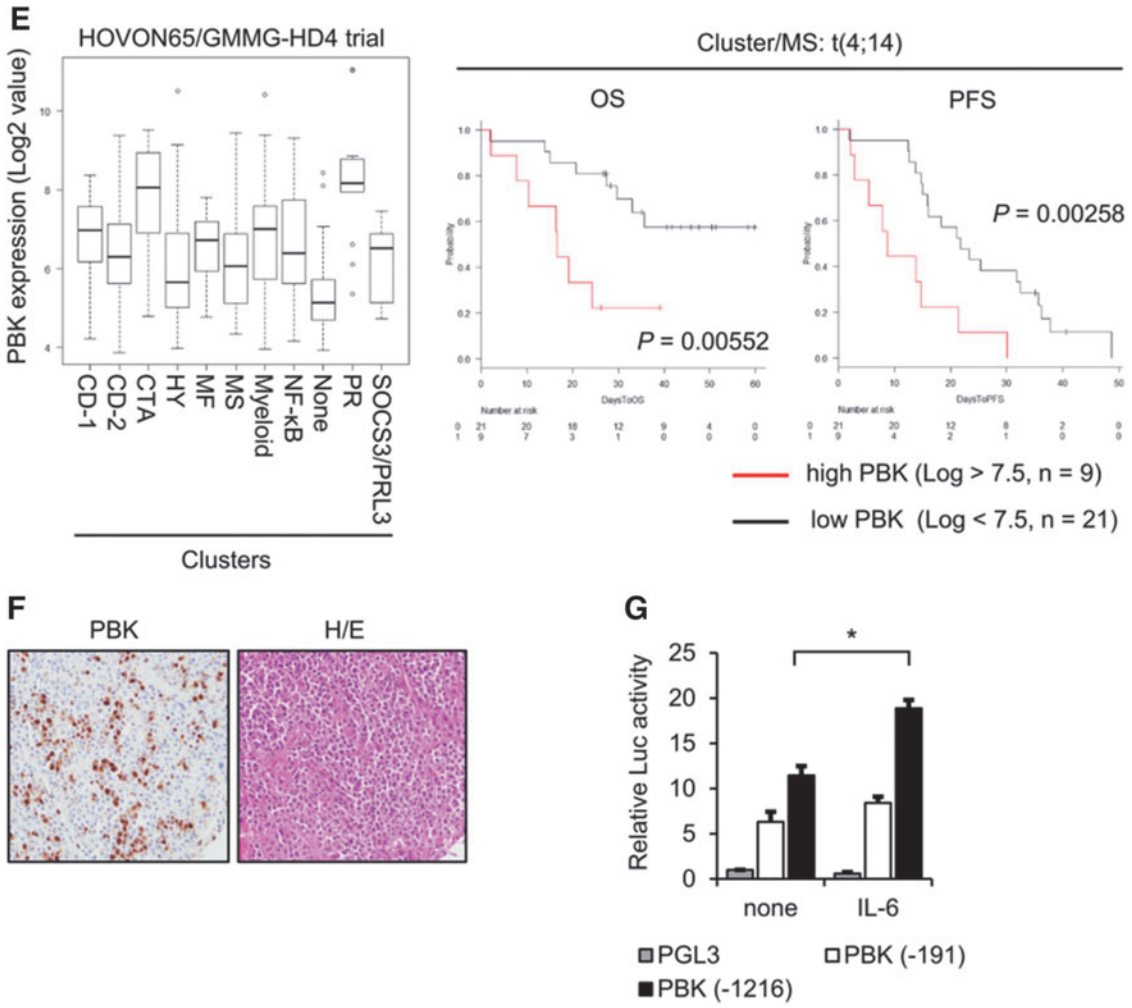

FIG. 1. (*Continued*).

also detected strong mRNA expression of PBK in IL-6-independent MM cell lines (Fig. 1B). Furthermore, Western blot analysis showed that PBK expression increased in IL-6-treated ANBL-6 and FLAM-76 cells, whereas strong PBK expression was detected in a subset of MM cell lines but not in bone marrow-derived CD138-negative cells (Fig. 1C). We also observed that in both IL-6-treated MM cells and IL-6-independent cell lines, where PBK expression was detected, phosphorylation levels of both Stat3 and Erk (p44/42) concomitantly increased (Fig. 1C). To further validate the expression of PBK in MM, a public cohort of 290 patients, HOVON-65/GMMG-HD4 (GSE19784) was analyzed (Supplementary Table S3) (Kuiper and others 2012; Broyl and others 2010). According to the $\log_2$ value of PBK probe (219148_at), patients were divided into 2 groups: high ($\log_2$ value >7.5, $n=62$) and low ($\log_2$ value <7.5, $n=228$) PBK expression. Of note, high PBK expression was significantly associated with both OS ($P=0.0000363$) and progression-free survival (PFS; $P=0.000519$) (Fig. 1D), PBK expression may be associated with tumor growth of MM. To further define the impact of PBK expression on disease progression, OS, and PFS, we examined the association between PBK expression and the International Staging System (ISS) or the gene cluster groups in the HOVON trial using statistical analyses. We found that PBK expression levels significantly increased in ISS stage II ($P=0.047$) and stage III ($P=0.011$) compared with ISS stage I (Table 2), which suggests that PBK expression may be associated with disease progression of MM. In addition, the Kruskal–Wallis test with 11 gene expression clusters revealed that high PBK expression is observed in the clusters of cancer testis antigens (CTA) and the proliferation-associated genes (PR) (Supplementary Table S4 and Fig. 1E). Importantly, we found that high PBK expression was significantly associated with both OS ($P=0.00552$) and PFS ($P=0.00258$) in the MS cluster showing translocation t(4;14), which is one of the prognostic parameters of patients with MM. In addition, we found that high PBK expression was significantly associated with PFS ($P=0.0254$) in the MF cluster showing translocation t(14;16) or t(14;20) (Supplementary Fig. S2). Furthermore, one-way analysis of variance showed that PBK expression is significantly associated with the ISS stages in the MS groups, but not other groups (I versus III, $P=0.0056$; Supplementary Fig. S2). These results indicate that PBK expression may have significant impact as a poor prognostic marker and may be independent from other prognostic parameters, such as t(4;14). We next examined the protein expression of PBK in MM using immunohistochemistry and

Western blot analysis. Immunohistochemistry showed that PBK expression was specifically detected in the $PBK^{+/+}$ KMS-11 cells but not in the genetically modified $PBK^{-/-}$ KMS-11 cells (Supplementary Fig. S3). Immunohistochemistry showed that PBK expression was detectable in both nucleus and cytoplasm of myeloma cells in the tissues of MM patients (Fig. 1F). Our database analysis showed that chromosomal copy number in *PBK* gene locus increased in the series of MM cell lines (gain, 23%; Supplementary Fig. S4). Furthermore, luciferase reporter gene assay showed that IL-6 treatment significantly increased *PBK* promoter activity in ANBL-6 cells expressing PBK (-1216)-luciferase (luc) but not in cells expressing PBK (-191)-luc and control luc (Fig. 1G). These results suggest that *PBK* gene expression could be induced by stimulation of IL-6 in MM cells.

Disruption of PBK expression suppresses tumor cell growth in vitro *and* in vivo

Since our analysis of clinical data suggests that PBK might be involved in tumor progression, we examined the effect of *PBK* expression on MM cell growth both *in vitro* and *in vivo*. We generated *PBK* knockout ($PBK^{-/-}$) cell clones using a MM cell line KMS-11 and CRISPR/Cas9 system by targeting PBK exon3 (Fig. 2A). Our strategy successfully disrupted *PBK* gene and generated 2 independent cell clones (Fig. 2A). Western blot analysis showed high PBK expression in parental KMS-11 cells but not in $PBK^{-/-}$ cell clones (Fig. 2B). Using the generated clones, we assessed the cell proliferation and clonogenicity by MTT assay, colony formation assay, and adherent-independent soft-agar colony formation assay. We found that cell proliferation was significantly suppressed (data not shown), the number of colonies significantly decreased (Fig. 2C), and the size of colonies and cell proliferation were highly reduced (Fig. 2D, E) in the $PBK^{-/-}$ cell clones compared with parental KMS-11 cells. Therefore, we next performed xenograft experiments using immunodeficient SCID mice to examine the effect of PBK on tumor growth *in vivo*. Of note, the tumor volume substantially reduced in the $PBK^{-/-}$ KMS-11 cell-derived tumor (Fig. 2F), compared with the $PBK^{+/+}$ KMS-11 cell-derived tumor. Moreover, rescuing PBK expression in $PBK^{-/-}$ KMS-11 cells significantly increased the number of colonies *in vitro* (Fig. 2G). These results strongly suggest that PBK might play an important role in the tumor growth of MM.

Loss of PBK rather than its genotype is associated with tumor growth of MM

Human *PBK* gene possesses single nucleotide polymorphism (SNP) rs3779620, which accompanies with an amino acid change from asparagine (A320, N107) to serine (A320G, N107S). Allele frequencies of A/A and A/G occupy more than 97% in both United States and Europe populations, while less than is 86% in Asian populations (Supplementary Table S5). Since the *PBK*/rs3779620 genotype of KMS-11 is a rare allele G/G, we sought to examine the effect of *PBK*/rs3779620 genotype on tumor growth of MM cells. To this end, we generated *PBK* gene knockin cell model using a MM cell line OCI-My5 (A/A at rs3779620) by targeting *PBK* Exon-5. Subsequently, CRISPR/Cas9-mediating genome editing successfully established $PBK^{A/A}$, $PBK^{G/G}$, and $PBK^{-/-}$ cell clones (Fig. 3A). Western blot analysis showed PBK protein expression in both the $PBK^{G/G}$ and $PBK^{A/A}$ cell clones but not in the $PBK^{-/-}$ OCI-My5 cell clone (Fig. 3B). Therefore, we examined the effect of *PBK* genotype on tumor growth using the cell clones *in vivo* and found that the rates of tumor engraftment as well as tumor growth were not significantly but slightly different between $PBK^{G/G}$ and $PBK^{A/A}$ cell clones (increased in $PBK^{A/A}$), whereas tumor growth of $PBK^{-/-}$ OCI-My5 cell-derived tumor was greatly suppressed compared with those of both $PBK^{G/G}$ and $PBK^{A/A}$ cell clones (Fig. 3C). This result suggests that PBK expression, rather than a *PBK* genotype rs3779620, may be closely associated with tumor growth of MM cells. It might be also important to note that allele frequencies of A/A occupy 90% in the MM cell lines used in this study (Supplementary Table S6).

Disruption of PBK increases apoptosis of MM cells

Since loss of *PBK* expression greatly reduced tumor growth of MM cells, we hypothesized that inhibition of PBK expression might be involved in the survival of MM cells. To examine the effect of PBK expression on apoptosis, we performed the Annexin V/PI double staining-based flow cytometry analysis using $PBK^{+/+}$ and $PBK^{-/-}$ MM cell clones. To this end, we additionally established the $PBK^{-/-}$ cell clone using a human MM cell line RPMI8226 (Supplementary Fig. S5a, b). We found that proliferation was slightly, but not significantly, slower in both the $PBK^{-/-}$ RPMI8226 (84.1% ± 1.7 at day 6, $P < 0.05$; 90.1% ± 1.9% at

Table 2. Relationship Between Clinical Characteristics and Gene Expression of PDZ-Binding Kinase in the HOVON-65/GMMG-HD4 Clinical Trial

			PBK *gene expression (Log_2 value)*						
		N	*Low*	%	*High*	%	*Ave.*	*SD*	P
Total		290	228	78.6	62	21.4	6.40	1.44	
ISS	I	114	98	86.0	16	14.0	6.10	1.36	
	II	71	52	73.2	19	26.8	6.61	1.34	0.047 (versus I)
	III	78	56	71.8	22	28.2	6.70	1.53	0.011 (versus I)
	NA	27	22	81.5	5	18.5	6.23	1.56	

PBK expression low, $\log_2$ <7.5; PBK expression high, $\log_2$ >7.5. The statistical analysis was performed using one-way ANOVA with pairwise comparison (Turkey).

ANOVA, analysis of variance; ISS, International Staging System; NA, not analyzed; PBK, PDZ-binding kinase; SD, standard deviation.

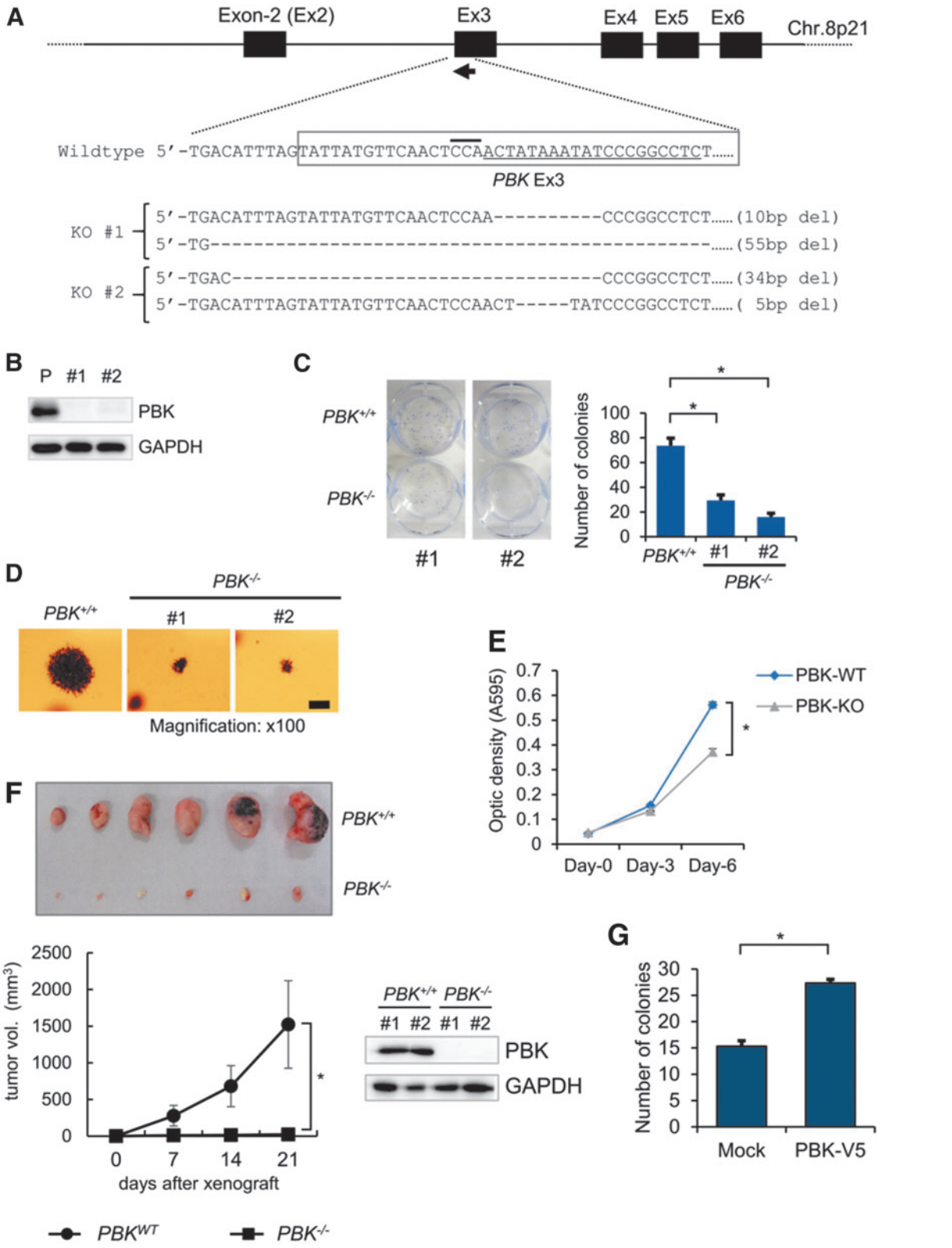

FIG. 2. The effect of PBK on the tumor growth in KMS-11 cells. **(A)** An sgRNA (*arrow*) sequence was designed against the *PBK* loci to excise an in-frame sequence of exon 3 (*gray restriction box*). The sgRNA sequence and the PAM sequence are indicated by an *underline* or *overbar*, respectively. **(B)** PBK protein expression was determined by Western blot analysis. GAPDH was used as an internal control. **(C)** Anchorage-dependent colony formation assay. *Bar graph* represents the number of stained colonies. Data are presented as the mean ± SE ($n = 3$). **(D)** Anchorage-independent soft-agar colony formation assay. **(E)** MTT assay was performed to examine the effect of PBK disruption on cell proliferation ($n = 3$). **(F)** Xenograft experiment. Twenty million KMS-11/$PBK^{+/+}$ and KMS11/$PBK^{-/-}$ cells were subcutaneously injected in the backside of female SCID mice ($n = 6$). **(G)** The effect of exogenous PBK expression on the proliferation of KMS-11 cells. Anchorage-dependent colony formation assay was performed as described in **(C)**. An *asterisk* (*) indicates statistically significant difference at $P < 0.05$. GAPDH, glyceraldehyde-3-phosphate dehydrogenase; MTT, Thiazolyl Blue Tetrazolium Bromide; SCID, severely compromised immunodeficient; SE, standard error; sgRNA, single guide RNA.

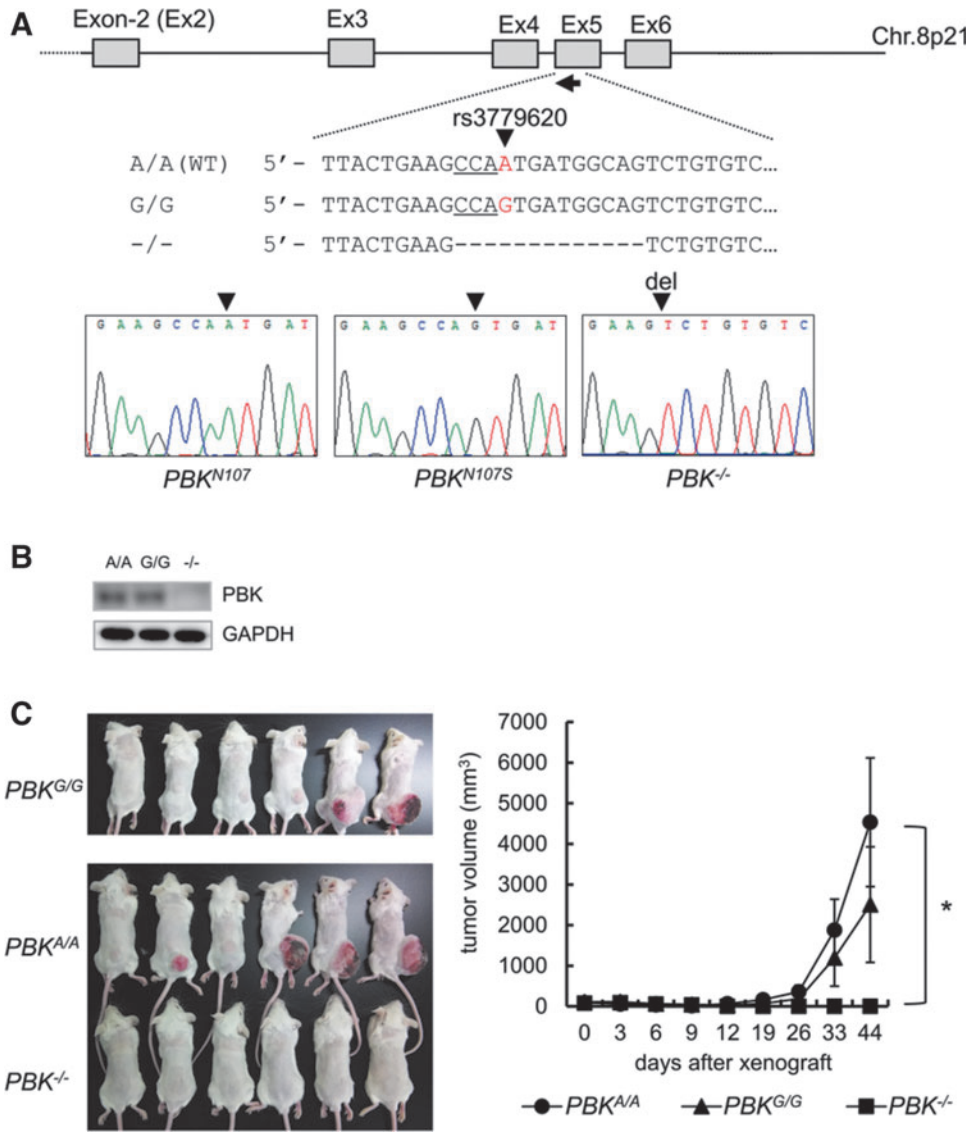

FIG. 3. Effect of PBK expression and its genotype rs3779620 on the tumor growth in OCI-My5 cells. **(A)** An sgRNA (*arrow*) sequence was designed against the *PBK* loci to excise and/or replace an in-frame sequence of Exon 5. The rs3779620 SNP and the PAM sequence are indicated by a *red character* (A or G) or *underline*, respectively. The sequences of the PBK^{N107}, PBK^{N107S}, and $PBK^{-/-}$ (null) OCI-My5 cell clones were analyzed, and the results are shown below. **(B)** PBK protein expression was determined by Western blot analysis. **(C)** Xenograft experiment. Twenty million PBK^{N107}, PBK^{N107S}, and $PBK^{-/-}$ (null) cells were subcutaneously injected in the backside of female SCID mice. The tumor growth was measured twice a week and the tumor volume (mm^3) was calculated by means of the modified ellipsoid formula 1/2 (length × $width^2$). An *asterisk* (*) indicates statistically significant difference at $P < 0.05$ ($n = 6$). SNP, single nucleotide polymorphism.

day 3, not significant, compared WITH $PBK^{+/+}$ cells) and OCI-My5 cells (51% ± 1.2% at day 3; 92.7% ± 1.6% at day-6, $P < 0.05$, compared with $PBK^{+/+}$ cells) (Supplementary Fig. S5c). We also performed an adherent-independent soft-agar colony formation assay, and found that colony size is reduced in the $PBK^{-/-}$ OCI-My5 clone compared with $PBK^{A/A}$ and $PBK^{G/G}$ OCI-My5 clones. In contrast, there are almost no differences in colony size between $PBK^{-/-}$ and $PBK^{+/+}$ RPMI8226 clones (Supplementary Fig. S5d). Interestingly, FACS analysis showed that the number of AxV^+/PI^+ cells significantly increased in the $PBK^{-/-}$ KMS-11 and RPMI8226 cell clones compared with $PBK^{+/+}$ cells (Fig. 4A). In addition, caspase-3/7 assay showed that the relative caspase-3/7 activities significantly increased in the $PBK^{-/-}$ RPMI8226 and OCI-My5 cell clones compared with the $PBK^{+/+}$ cells (Fig. 4B). Furthermore, PI staining-based cell cycle analysis showed that the percentage of sub-G1 population increased in all the $PBK^{-/-}$ KMS-11 and RPMI8226 cell clones compared with those in $PBK^{+/+}$ cells (Fig. 4C). These results suggest that PBK expression might be related to the survival of MM cells.

PBK expression is associated with Stat3 phosphorylation level and IL-6-Stat3 signaling axis

We next examined the effect of *PBK* disruption on cellular signaling in MM cells using Western blot analysis. Of note, phosphorylation levels of Stat3 highly decreased in the $PBK^{-/-}$ KMS-11 and OCI-My5 cells compared with that in $PBK^{+/+}$ cells (Fig. 5A). In contrast, no significant changes in the phosphorylation levels of MAPKs and Akt, Myc protein expression, and *IRF4* mRNA expression were observed in the RPMI8226 and KMS-11 cell clones (Supplementary Figs. S5b and S6A, B). We also found that β-catenin, the activity of which was reported to be associated with PBK expression, decreased in the $PBK^{-/-}$ OCI-My5 and RPMI8226 cell clones compared with wild-type (WT) cell clones. (Supplementary Fig. S7a). Since Stat3 signaling confers resistance to apoptosis in MM cells (Catlett-Falcone and others 1999), we examined the effect of exogenous PBK expression on the phosphorylation of Stat3. To this end, we generated cells expressing lentivirus-based PBK tagged with V5 in the $PBK^{-/-}$ KMS-11 and OCI-My5 cells. Western blot analysis showed that the phosphorylation levels of Stat3

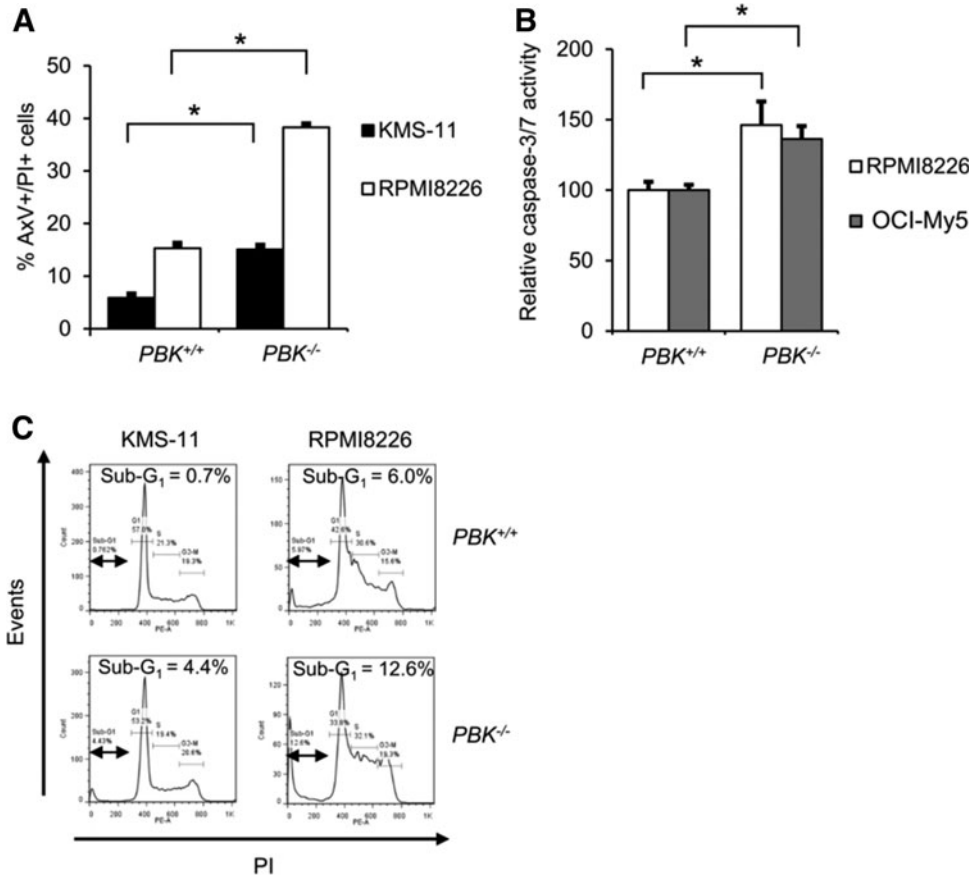

FIG. 4. Effect of PBK expression on apoptosis of MM cells. **(A)** Flow cytometry analysis of MM cell lines using double staining with Annexin V (Ax-FITC) and PI. $PBK^{+/+}$ and $PBK^{-/-}$ MM cells were seeded and incubated for 48 h. *Bar graphs* show the percentage of apoptotic (AxV^+/PI^+) cells. **(B)** Effect of PBK expression on caspase-3/7 activity. Data are expressed relative to caspase-3/7 activity in control cells ($PBK^{+/+}$ cells), which was arbitrarily set at 100%. Data are also expressed as the mean ± SE ($n = 3$) (*$P < 0.05$). **(C)** Effect of PBK expression on the sub-G1 population of the cell cycle. The percentages show the ratio of the sub-G1 population. PI, propidium iodide.

(Tyr705) clearly increased in the $PBK^{-/-}$ cells expressing PBK-V5 compared with the control cells (Fig. 5B). To investigate whether phosphorylation of PBK itself affects PBK-induced phosphorylation of Stat3, we transiently transfected EGFP-PBK^{WT} or EGFP-PBK^{T9A} mutant in 2 other human MM cell lines U266 and UTMC-2. Western blot analysis showed that the phosphorylation of Stat3 increased in cells expressing either EGFP-PBK^{WT} or EGFP-PBK^{T9A} compared with cells expressing EGFP alone (Fig. 5C). To examine whether pharmacologic inhibition of Stat3 recapitulates silencing of PBK, we examined the effects of SH4–54 on PBK expression in IL-6-independent MM cell lines. This assay showed that PBK expression readily decreased concomitantly with phosphorylation levels of Stat3 in RPMI8226, UTMC-2, and OCI-My5 cells (Supplementary Fig. S7b). This suggests that Stat3 signaling may play an important role in PBK expression in IL-6-independent MM cells. To further investigate whether PBK kinase activity and/or PDZ-binding domain was related to the phosphorylation of Stat3, we transiently transfected EGFP-PBK^{WT}, kinase dead mutant EGFP-$PBK^{K64A,K65A}$, or EGFP-PBK^{K320A} mutant into U266 cells. Interestingly, increased phosphorylation of Stat3 was observed in cells expressing EGFP-PBK^{K320A} as well as in EGFP-PBK^{WT}, but not in cells expressing EGFP-$PBK^{K64A,K65A}$ (Fig. 5D). Moreover, GSEA analysis of Hallmark gene sets in the $PBK^{-/-}$ KMS-11 cells and their xenografted tumor demonstrated significant downregulation of genes related to IL-6-Stat3 signaling both *in vitro* and *in vivo*, whereas no significant changes in the Wnt-β-catenin signaling pathway (Fig. 5E and Supplementary Table S7). Since our GSEA showed downregulation of genes related to IL-6-Stat3 signaling in $PBK^{-/-}$ KMS-11 cells, we hypothesize that decreases in CD130 (IL6ST) expression may lead to a decrease in IL-6 signaling, and a subsequent decrease in phosphorylation of Stat3. Pearson's correlation analysis revealed that there is a low, but significant, negative correlation between PBK and CD130 expression in a public cohort of 290 patients, HOVON-65/GMMG-HD4 ($r = -0.128$, $P < 0.03$; Supplementary Fig. S8). Gene expression analysis showed that the disruption of PBK does not alter the expression levels of other IL-6-related molecules, such as CD130, oncostatin M (OSM), IL-11, and leukemia inhibitory factor (LIF) (Supplementary Fig. S9). These results strongly suggest that PBK expression and its kinase activity may be related to the phosphorylation of Stat3.

To examine the effects of anti-MM drugs, such as bortezomib (BOR), lenalidomide (LEN), and pomalidomide (POM), on the survival of $PBK^{-/-}$ MM cells, an MTT assay was used. The MTT assay showed that cell survival percentages significantly increased after BOR treatment in the $PBK^{-/-}$ KMS-11 and OCI-My5 cells (Supplementary Fig. S10A), whereas they were not altered after treatment with either LEN or POM (Supplementary Fig. S10B, C).

A specific PBK inhibitor OTS514 suppresses KMS-11-induced tumor cell growth in vivo

Since knockout of *PBK* dramatically reduced tumor growth of MM cells *in vivo*, we examined the effect of a novel PBK-specific inhibitor OTS514 on KMS-11-induced tumor growth *in vivo*. The xenografted mice were intraperitoneally injected

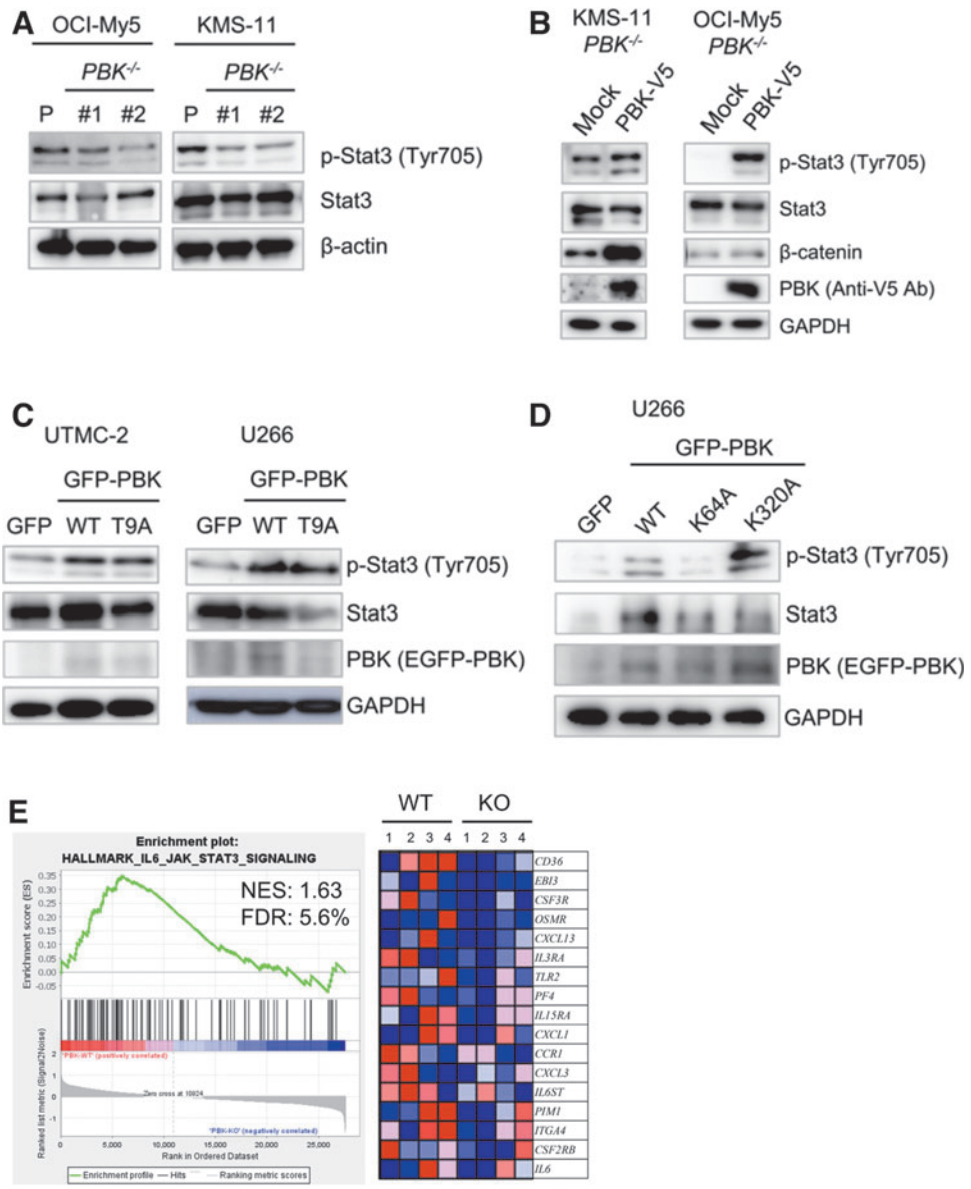

FIG. 5. The effect of PBK expression on cellular signaling in MM cells. **(A)** *PBK*$^{+/+}$ and *PBK*$^{-/-}$ KMS-11 cells were seeded and incubated for 48 h. **(B)** The effect of exogenous PBK expression on the phosphorylation level of Stat3 in *PBK*$^{-/-}$MM cells. Lentivirus-induced PBK expression was confirmed by Western blot analysis by using anti-V5 tag antibody. **(C, D)** The effect of transient expression of PBK and its mutant PBK^{T9A} on the phosphorylation level of Stat3. **(C)** EGFP-C1 (GFP), PBK/EGFP-C1 (WT), or PBK ^{T9A}-EGFP vectors were introduced into the human myeloma cell lines UTMC-2 and U266 by using nucleofection method. **(D)** EGFP-C1 (GFP), PBK/EGFP-C1 (WT), or kinase dead mutant PBK ^{K64A}-EGFP-C1 or ΔPDZ-binding domain mutant PBK^{K320A}/EGFP-C1 vectors were introduced into U266 cells as described above. **(E)** GSEA. GSEA was conducted using GSEA v4.0.2 software and Molecular Signatures Database (Broad Institute). All raw data were formatted and applied to hallmark gene sets (h.all.v7.0). Genes contributing to enrichment are shown in *rows*, and the sample is shown in 1 column on the heatmap. Expression level is represented as a gradient from high (*red*) to low (*blue*). Lanes 1–2, expression levels in cultivated cells *in vitro*; lanes 3–4, expression levels in tumors *in vivo*. FDR, false discovery rate; GSEA, gene set enrichment analysis; NES, normalized enrichment score; WT, wild type.

with vehicle (saline solution) or OTS514 (10 mg/kg) every 2 days, until the volume of each tumor reached from 400 to 500 mm^3. Interestingly, intraperitoneal injection of OTS514 (10 mg/kg) significantly suppressed the tumor growth, compared with vehicle treatment (Fig. 6A, B). Additionally, no significant loss of body weight was observed in mice treated with OTS514 (Fig. 6C). Western blot analysis showed that the phosphorylation levels of Stat3 and β-catenin decreased in the OTS514-injected tumors compared with the vehicle-injected tumors (Fig. 6D). Furthermore, the expression of cleaved PARP increased in the OTS514-treated tumors compared with the vehicle-treated tumors (Fig. 6D). Similar results were observed *in vitro* when KMS-11 and OCI-My5 cells were treated with OTS514 (Fig. 6E). Collectively, these results strongly indicate the possibility that PBK plays an important role in the tumor growth of MM cells.

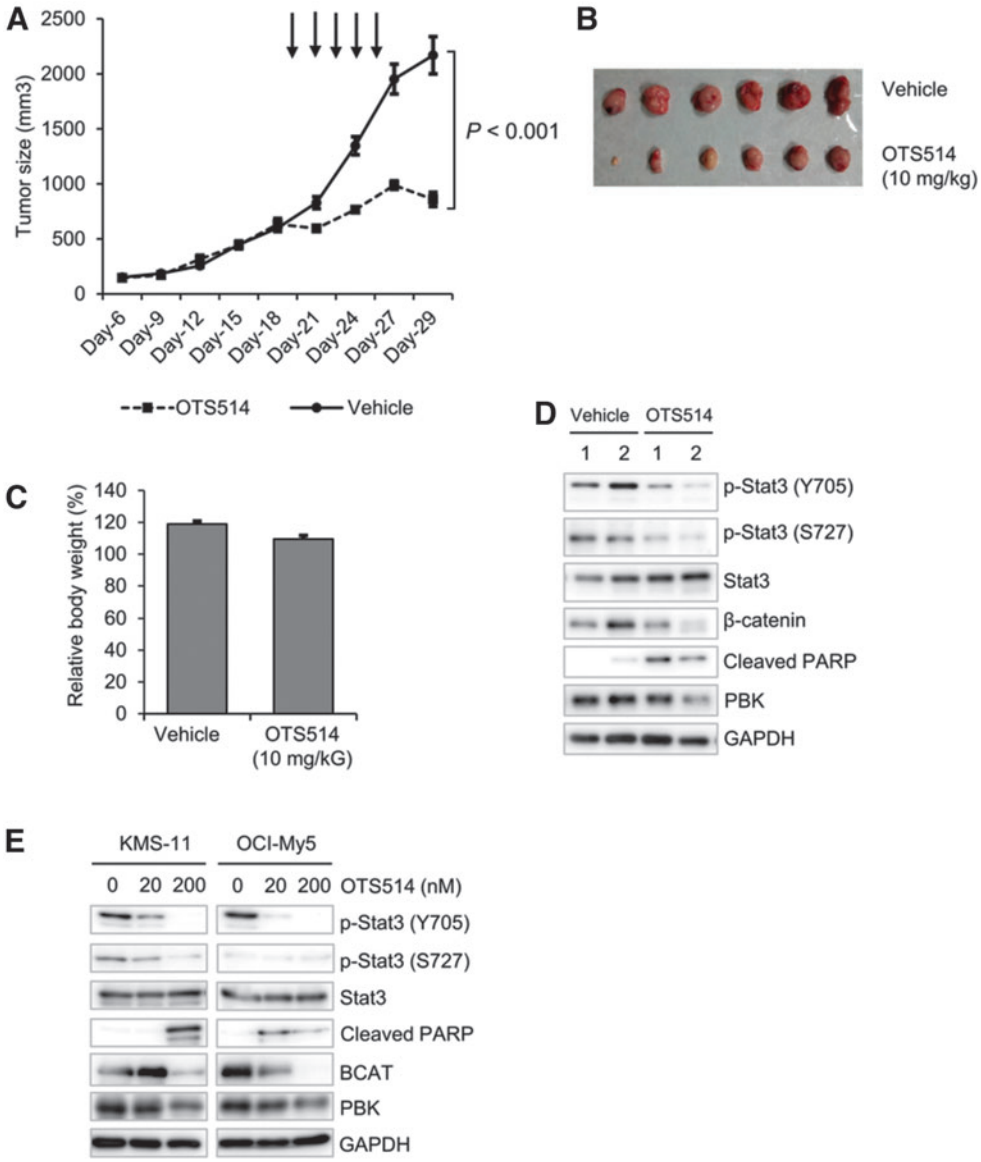

FIG. 6. The effect of PBK inhibitor OTS514 on KMS-11 cell-derived tumor growth. **(A)** Each *line graph* shows tumor volume during chemotherapy. The *arrows* indicate time points of administration of OTS514 intraperitoneally into the xenografted mice. **(B)** A representative picture of tumor in each group is shown. **(C)** *Bar graph* shows the changes in body weight of mice after chemotherapy. For normalization, data were expressed relative to percentage of body weight in mice before treatment, which was arbitrarily set at 100%. **(D, E)** Protein expression levels of phospho-Stat3, Stat3, β-catenin and cleaved PARP in **(D)** KMS-11-derived tumors and cultured **(E)** KMS-11 and OCI-My5 cells. KMS-11 and OCI-My5 cells were treated with the indicated concentrations of OTS514 (0, 20, 200 nM) for 24 h *in vitro*.

Discussion

The clinical outcome of patients with MM has gradually improved due to the advent of new classes of anti-MM drugs. Oncologists are expecting to achieve further improvement in novel therapeutics, such as combinatorial strategies with recently developed antibody-based and/or immune-based therapies. Despite such advances in therapeutic strategies, the clinical outcome of patients with MM remains incurable. The present study is the first to report that high PBK expression is associated with shorter survival of patients with MM. We found that disruption of the *PBK* gene dramatically reduced tumor growth of MM cells both *in vitro* and *in vivo*, regardless of its genotype rs3779620. Furthermore, a specific PBK inhibitor, OTS514, significantly suppressed growth of KMS-11-derived tumor without causing body weight loss. Mechanistically, the number of apoptotic cells was observed to increase in $PBK^{-/-}$ MM cells with concomitant increase in caspase-3/7 activity. Moreover, the phosphorylation level of Stat3 decreased in $PBK^{-/-}$ MM cells, whereas it increased following expression of WT PBK but not kinase-dead PBK.

Upregulation of PBK expression has been reported in several types of solid cancers, including esophageal squamous cell carcinoma, gastric carcinoma, prostate carcinoma, oral cancer, glioma, and ovarian cancer (Matsuo and others 2014; Brown-Clay and others 2015; Chang and others 2016; Ikeda and others 2016; Kwon and others 2016; Ohashi and others 2016, 2017; Quan and others 2017; Yang and others 2017). Yang and others (2017) recently reported that increased PBK expression was associated with larger tumor size, presence of vascular invasion, lymph node metastasis, and poor overall and disease-free survival in two independent cohorts of 879 patients with hepatocellular carcinoma. Ohashi and others (2016, 2017) reported that overexpression of PBK/TOPK contributes to tumor development and poor outcome of both esophageal squamous cell carcinoma and gastric cancer. It has also been reported that PBK expression was related to high recurrence of prostate cancer (Chen and others 2015). In this study, we found that high expression level of PBK was significantly associated with both OS and PFS of patients with MM. We also showed that loss of PBK dramatically decreased the tumor growth of MM cells

using a xenograft model. These results suggest that PBK expression level is closely associated with tumor malignancies in patients with MM.

On the other hand, our MTT assay showed that the cell survival percentage significantly increased after treatment with anti-MM drug BOR in the $PBK^{-/-}$ OCI-My5 and RPMI8226 cells. Since bortezomib inhibits proteasome activity, PBK expression may be associated with proteasome activity, which is activated in MM cells (Edwards and others 2009). Additional studies to assess the relationship between drug susceptibilities of patients with MM and PBK expression are needed to understand the involvement of PBK in the progression and pathogenesis of MM in clinical settings.

The molecular mechanism by which cancerous cells regulate the expression of PBK is still obscure. Hu and others (2013) reported that c-Myc and E2F1 drive PBK/TOPK expression in high-grade malignant lymphomas. In this study, we found that IL-6 increased PBK expression at both the mRNA and protein levels in IL-6-dependent MM cell lines. Our reporter gene assay showed that IL-6 treatment significantly increased the PBK promoter activity, suggesting that PBK may be a novel IL-6-inducible gene in MM cells. We showed that the number of apoptotic cells significantly increases in the $PBK^{-/-}$ RPMI8226 clone compared with the $PBK^{+/+}$ clone, and we did not observe a significant growth delay in RPMI8226 cells, which lacks t(4;14). Based on our data, along with the public cohort that shows that PBK expression is significantly associated with poor prognosis in MM patients with t(4;14), it is possible that the involvement of PBK in tumor growth is more obvious in MM cells with t(4;14). The t(4;14) translocation is known to cause the concomitant overexpression of 2 genes, fibroblast growth factor receptor 3 (*FGFR3*) and multiple myeloma SET domain (*MMSET*), both of which exert growth advantage effects (Keats and others 2003, 2005; Santra and others 2003; Huang and others 2018). As such, PBK may cooperate with FGFR3 and/or MMSET to promote tumor growth of MM cells. Further studies are required to elucidate the relationship between PBK-induced tumor cell growth and chromosomal abnormalities in MM cells. Increased PBK expression was observed in IL-6-independent MM cell lines. In this study, we showed that the Stat3 inhibitor SH4-54 decreases PBK expression, whereas the PBK inhibitor OTS514 and PBK depletion decrease phosphorylation levels of Stat3 in the MM cells. In addition, our GSEA revealed that IL-6-Jak-Stat3 signaling is significantly inactivated in the $PBK^{-/-}$ KMS-11-derived tumors. These results indicate that PBK expression may form a positive feed-forward regulation with Stat3 to promote tumor growth of MM. PBK was initially identified as a serine/threonine MAPK kinase (MAPKKs) with similarities to MEK1/2 (Abe and others 2000), which could phosphorylate Stat3 at Ser727 (Lim and Cao, 2001; Huang and others 2014). Our data on OTS514 suggest decreased phosphorylation of Stat3 at Ser727, whereas our data on Tyr705 suggest that PBK may regulate Stat3 activity by modulating Stat3 phosphorylation. Additional studies are required to understand whether PBK is directly involved in the phosphorylation of Stat3. We also found that the genomic copy number of the *PBK* locus at chromosome 8q21.1 increased in human MM cell lines, including KMS-11 with high PBK expression, whereas there is no correlation between the copy number of the *PBK* gene locus and protein expression levels in U266 and RPMI8226 cells. Therefore, it could be possible that PBK overexpression is partly caused by gene amplification.

Stat3 plays a pivotal role in the survival of MM cells (Takeda and others 1997; Alas and Bonavida 2003; Bharti and others 2004; Brocke-Heidrich and others 2004; Jung and others 2017; Huang and others 2018). Our data showed that knockout of *PBK* expression decreased, and rescue of its expression in $PBK^{-/-}$ cells increased the phosphorylation level of Stat3. In addition, the phosphorylation of Stat3 was suppressed by OTS514 treatment both *in vitro* and *in vivo*. Furthermore, WT PBK, but not its kinase dead mutant $PBK^{K64AK65A}$, increased Stat3 phosphorylation. We also found that loss of *PBK* significantly increased caspase-3 activity as well as the number of apoptotic cells. Recently, Ohashi and others (2016) reported that PBK knockdown increases both early and late apoptotic cells in *TP53*-mutated —but not *TP53*-intact—esophageal squamous cell carcinoma cells. Since patients with biallelic inactivation of the *TP53* gene showed poor prognosis in patients with MM (Shah and others 2018), it is preferable to utilize a PBK inhibitor to treat patients with a biallelic loss of *TP53* in clinical settings. It has been reported that PBK exerts oncogenic activity in hepatocellular carcinoma cells through activation of the beta-catenin signaling pathway (Yang and others 2017). Thus, we examined the effects of PBK disruption on beta-catenin expression in MM cells. A Western blot analysis showed that beta-catenin expression readily decreased in $PBK^{-/-}$ MM cells, whereas GSEA showed no significant changes in the expression levels of genes that are related to beta-catenin in the KMS-11-derived tumors. These results suggest that the PBK-Stat3 axis is more likely to be associated with PBK-induced tumor growth of MM. These results strongly suggest that PBK and Stat3 may cooperatively regulate the survival of MM cells.

In this study, we showed that the frequencies of nonsynonymous SNP rs3779620 in the *PBK* gene varies among ethnic groups. We generated isogenic gene knockin MM cell clones and examined the effects of the *PBK* genotype rs3779620 on tumor growth of OCI-My5 *in vivo*. Our xenograft experiment showed that the tumor growth of $PBK^{-/-}$ OCI-My5 cell-derived tumors was greatly suppressed compared with those of both $PBK^{G/G}$ and $PBK^{A/A}$ cell clones, whereas the tumor growth rate of $PBK^{A/A}$ cells was insignificantly but slightly higher compared with $PBK^{G/G}$. Given our finding that decreased $PBK^{G/G}$ KMS-11 cells and $PBK^{A/A}$ in OCI-My5 cells greatly decreases tumor growth, PBK expression may play an important role for tumor growth of MM. Additional studies are needed to clarify the association of rs3779620 with tumor progression and/or drug susceptibility in MM cells.

It has been recently reported that oral administration of the specific PBK inhibitor, OTS514, prolongs OS in human ovarian cancer abdominal dissemination xenograft model (Ikeda and others 2016). Another PBK inhibitor, HI-TOPK-032, suppressed tumor growth in a colon cancer xenograft model (Kim and others 2012). In this study, we showed that intraperitoneal administration of OTS514 significantly suppressed tumor cell size in the xenograft model developed using the human MM cell line, KMS-11. Importantly, administration of OTS514 did not result in significant loss of

body weight in xenografted mice used in this study. However, Matsuo and others (2014) have reported that OTS514 potentially causes certain toxicity in hematopoiesis. They also showed that liposomal OTS964, a demethylated derivative of OTS514, exhibits favorable antitumor activity without any toxicities in the xenograft (Matsuo and others 2014). Although our data did not show the severe toxicity of OTS514 *in vivo*, it might be a better option to utilize liposomal OTS964 to gain the antimyeloma effect by mediating inhibition of PBK activity. Hence, data suggest that the antiproliferative effect of OTS514 may preferentially act toward tumorigenic cells. On the other hand, Lin and others (2019) reported the off-target effects of OTS514, which preferentially target the kinase activity of the cyclin-dependent kinase 11 (CDK11)). In this study, our finding that $PBK^{-/-}$ MM cells are more sensitive to treatment with OTS514 indicates that molecular targets of OTS514 may not always be restricted to only PBK (Supplementary Fig. S11). Thus, it would be interesting to compare the antitumor effects of OTS514 between $PBK^{+/+}$ and $PBK^{-/-}$ cells *in vivo*.

This study has some limitations. First, most of our observations were obtained from a single MM cell line, KMS-11. Second, our data does not always explain the detailed molecular mechanism by which PBK loss decreases tumor growth of MM cells. Third, the PBK inhibitor, OTS514, may exhibit an off-target effect in MM cells. Since PBK expression is inducible by IL-6, and is associated with the levels of phosphorylated Stat3, it is possible that PBK plays an important role in IL-6-Stat3 signaling, potentially cooperating with regulatory molecules, including PIAS proteins, SOCS proteins, phosphatases, and microRNAs (Johnson and others 2018).

In conclusion, this study is the first to demonstrate that high expression of PBK is closely associated with shorter survival of patients with MM, and promotes tumor growth of MM cells, at least in part, through enhancing cell survival with concomitant increase in the phosphorylation of Stat3. Although we have not utilized cells derived from primary MM patients, our results suggest that PBK expression could be a novel prognostic marker for patients with MM. Furthermore, compound treatment *in vivo* raises the interesting possibility that PBK inhibitor, OTS514, might have clinical potential as a novel therapeutic for patients with MM possessing high PBK expression. Additional studies are warranted to improve our understanding of the role of PBK in the pathophysiology of MM and to develop a novel molecular-targeted therapy for patients with relapsed or refractory MM.

Authors' Contributions

A.O. designed experiments, performed research, and wrote the article; I.H. designed research, analyzed data, and wrote the article; S.K. performed research; S.I. performed research and analyzed data of immunohistochemistry; N.T. performed research on gene expression analysis; V.Q.L. performed research and analyzed data; S.M. and J.K. contributed vital new reagents or analytical tools; M.W., M.L.R., and T.H. analyzed data.; H.K. wrote the article; S.T. designed experiments; H.I. analyzed data of immunohistochemistry; A.T. designed research; Y.H. designed experiments and edited the article.

Acknowledgments

The authors would like to thank Dr. M. Okumura for his assistance with animal care. They thank Mr. Makoto Naruse, Ms. Natsumi Kodama, and colleagues at the Division of Advanced Research Promotion, Institute of Comprehensive Medical Research at Aichi Medical University for providing their technical assistance. The authors appreciate Ms. K. Tanimizu for her technical assistance with immunohistochemistry. They also thank Ms. K. Hasegawa and Ms. A. Nakamura for their valuable secretarial assistances. They would like to thank Editage for English language editing.

Author Disclosure Statement

The authors declare no competing interests.

Funding Information

This work was partly supported by Grants-in-Aid for Scientific Research (KAKENHI) from the Japan Society for the Promotion of Science (15K19561 to A.O., 19K08825 to I.H., A.O., S.K., 18K08342 to A.O. and I.H., 17K07263 to H.K., S.K. and T.H.), the Research Grant from The Hori Science and Arts Foundation (to A.O.), YOKOYAMA Foundation for Clinical Pharmacology (YRY-1709 to A.O.), Nagao Memorial Fund (to A.O.), Japanese Society of Myeloma Research Award (to A.O.), Bristol-Myers Squibb (to I.H.), Celgene (A.O., I.H.), and The Japanese Society of Hematology Research Grant (I.H.).

Supplementary Material

Supplementary Figure S1
Supplementary Figure S2
Supplementary Figure S3
Supplementary Figure S4
Supplementary Figure S5
Supplementary Figure S6
Supplementary Figure S7
Supplementary Figure S8
Supplementary Figure S9
Supplementary Figure S10
Supplementary Figure S11
Supplementary Table S1
Supplementary Table S2
Supplementary Table S3
Supplementary Table S4
Supplementary Table S5
Supplementary Table S6
Supplementary Table S7

References

Abe Y, Matsumoto S, Kito K, Ueda N. 2000. Cloning and expression of a novel MAPKK-like protein kinase, lymphokine-activated killer T-cell-originated protein kinase, specifically expressed in the testis and activated lymphoid cells. J Biol Chem 275(28):21525–21531.

Abe Y, Takeuchi T, Kagawa-Miki L, Ueda N, Shigemoto K, Yasukawa M, Kito K. 2007. A mitotic kinase TOPK enhances Cdk1/cyclin B1-dependent phosphorylation of PRC1 and promotes cytokinesis. J Mol Biol 370(2):231–245.

Alas S, Bonavida B. 2003. Inhibition of constitutive STAT3 activity sensitizes resistant non-Hodgkin's lymphoma and multiple myeloma to chemotherapeutic drug-mediated apoptosis. Clin Cancer Res 9(1):316–326.

Anderson KC, Alsina M, Bensinger W, Biermann JS, Chanan-Khan A, Cohen AD, Devine S, Djulbegovic B, Faber EA, Jr., Gasparetto C, Huff CA, Kassim A, Medeiros BC, Meredith R, Raje N, Schriber J, Singhal S, Somlo G, Stockerl-Goldstein K, Treon SP, Tricot G, Weber DM, Yahalom J, Yunus F; National Comprehensive Cancer Network. 2011. Multiple myeloma. J Natl Compr Canc Netw 9(10):1146–1183.

Bharti AC, Shishodia S, Reuben JM, Weber D, Alexanian R, Raj-Vadhan S, Estrov Z, Talpaz M, Aggarwal BB. 2004. Nuclear factor-kappaB and STAT3 are constitutively active in $CD138^+$ cells derived from multiple myeloma patients, and suppression of these transcription factors leads to apoptosis. Blood 103(8):3175–3184.

Boyd KD, Ross FM, Chiecchio L, Dagrada GP, Konn ZJ, Tapper WJ, Walker BA, Wardell CP, Gregory WM, Szubert AJ, Bell SE, Child JA, Jackson GH, Davies FE, Morgan GJ; NCRI Haematology Oncology Studies Group. 2012. A novel prognostic model in myeloma based on co-segregating adverse FISH lesions and the ISS: analysis of patients treated in the MRC Myeloma IX trial. Leukemia 26(2):349–355.

Brocke-Heidrich K, Kretzschmar AK, Henze C, Löffler D, Koczan D, Thiesen HJ, Burger R, Gramatzki M, Horn F. 2004. Interleukin-6-dependent gene expression profiles in multiple myeloma INA-6 cells reveal a Bcl-2 family-independent survival pathway closely associated with Stat3 activation. Blood 103(1):242–251.

Brown-Clay JD, Shenoy DN, Timofeeva O, Kallakury BV, Nandi AK, Banerjee PP. 2015. PBK/TOPK enhances aggressive phenotype in prostate cancer via β-catenin-TCF/LEF-mediated matrix metalloproteinases production and invasion. Oncotarget 6(17):15594–15609.

Broyl A, Hose D, Lokhorst H, de Knegt Y, Peeters J, Jauch A, Bertsch U, Buijs A, Stevens-Kroef M, Beverloo HB, Vellenga E, Zweegman S, Kersten MJ, van der Holt B, el Jarari L, Mulligan G, Goldschmidt H, van Duin M, Sonneveld P. 2010. Gene expression profiling for molecular classification of multiple myeloma in newly diagnosed patients. Blood 116(14):2543–2553.

Catlett-Falcone R, Landowski TH, Oshiro MM, Turkson J, Levitzki A, Savino R, Ciliberto G, Moscinski L, Fernández-Luna JL, Nuñez G, Dalton WS, Jove R. 1999. Constitutive activation of Stat3 signaling confers resistance to apoptosis in human U266 myeloma cells. Immunity 10(1):105–115.

Chang CF, Chen SL, Sung WW, Hsieh MJ, Hsu HT, Chen LH, Chen MK, Ko JL, Chen CJ, Chou MC. 2016. PBK/TOPK expression predicts prognosis in oral cancer. Int J Mol Sci 17(7):1007.

Chen JH, Liang YX, He HC, Chen JY, Lu JM, Chen G, Lin ZY, Fu X, Ling XH, Han ZD, Jiang FN, Zhong WD. 2015. Overexpression of PDZ-binding kinase confers malignant phenotype in prostate cancer via the regulation of E2F1. Int J Biol Macromol 81:615–623.

Chng WJ, Dispenzieri A, Chim CS, Fonseca R, Goldschmidt H, Lentzsch S, Munshi N, Palumbo A, Miguel JS, Sonneveld P, Cavo M, Usmani S, Durie BG, Avet-Loiseau H; International Myeloma Working Group. 2014. IMWG consensus on risk stratification in multiple myeloma. Leukemia 28(2):269–277.

Edwards CM, Lwin ST, Fowler JA, Oyajobi BO, Zhuang J, Bates AL, Mundy GR. 2009. Myeloma cells exhibit an increase in proteasome activity and an enhanced response to proteasome inhibition in the bone marrow microenvironment *in vivo*. Am J Hematol 84(5):268–272.

Fujibuchi T, Abe Y, Takeuchi T, Ueda N, Shigemoto K, Yamamoto H, Kito K. 2005. Expression and phosphorylation of TOPK during spermatogenesis. Dev Growth Differ 47(9):637–644.

Gaudet S, Branton D, Lue RA. 2000. Characterization of PDZ-binding kinase, a mitotic kinase. Proc Natl Acad Sci U S A 97(10):5167–5172.

Hossain E, Ota A, Karnan S, Takahashi M, Mannan SB, Konishi H, Hosokawa Y. 2015. Lipopolysaccharide augments the uptake of oxidized LDL by up-regulating lectin-like oxidized LDL receptor-1 in macrophages. Mol Cell Biochem 400(1–2):29–40.

Hu F, Gartenhaus RB, Zhao XF, Fang HB, Minkove S, Poss DE, Rapoport AP. 2013. c-Myc and E2F1 drive PBK/TOPK expression in high-grade malignant lymphomas. Leuk Res 37(4):447–454.

Huang G, Yan H, Ye S, Tong C, Ying QL. 2014. STAT3 phosphorylation at tyrosine 705 and serine 727 differentially regulates mouse ESC fates. Stem Cells 32(5):1149–1160.

Huang YH, Molavi O, Alshareef A, Haque M, Wang Q, Chu MP, Venner CP, Sandhu I, Peters AC, Lavasanifar A, Lai R. 2018. Constitutive activation of STAT3 in myeloma cells cultured in a three-dimensional, reconstructed bone marrow model. Cancers (Basel) 10(6):206.

Iida S, Hanamura I, Suzuki T, Kamiya T, Kato M, Hayami Y, Miura K, Harada S, Tsuboi K, Wakita A, Akano Y, Taniwaki M, Nitta M, Ueda R. 2000. A novel human multiple myeloma-derived cell line, NCU-MM-1, carrying t(2;11)(q11;q23) and t(8;22)(q24;q11) chromosomal translocations with overexpression of c-Myc protein. Int J Hematol 72(1):85–91.

Ikeda Y, Park JH, Miyamoto T, Takamatsu N, Kato T, Iwasa A, Okabe S, Imai Y, Fujiwara K, Nakamura Y, Hasegawa K. 2016. T-LAK cell-originated protein kinase (TOPK) as a prognostic factor and a potential therapeutic target in ovarian cancer. Clin Cancer Res 22(24):6110–6117.

Jelinek DF, Ahmann GJ, Greipp PR, Jalal SM, Westendorf JJ, Katzmann JA, Kyle RA, Lust JA. 1993. Coexistence of aneuploid subclones within a myeloma cell line that exhibits clonal immunoglobulin gene rearrangement: clinical implications. Cancer Res 53(21):5320–5327.

Johnson DE, O'Keefe RA, Grandis JR. 2018. Targeting the IL-6/JAK/STAT3 signalling axis in cancer. Nat Rev Clin Oncol 15(4):234–248.

Jung SH, Ahn SY, Choi HW, Shin MG, Lee SS, Yang DH, Ahn JS, Kim YK, Kim HJ, Lee JJ. 2017. STAT3 expression is associated with poor survival in non-elderly adult patients with newly diagnosed multiple myeloma. Blood Res 52(4):293–299.

Kanda Y. 2013. Investigation of the freely-available easy-to-use software ''EZR'' (Easy R) for medical statistics. Bone Marrow Transplant 48(3):452–458.

Kawano M, Hirano T, Matsuda T, Taga T, Horii Y, Iwato K, Asaoku H, Tang B, Tanabe O, Tanaka H, Kuramoto A, Kishimoto T. 1998. Autocrine generation and requirement of BSF-2/IL-6 for human multiple myelomas. Nature 332(6159):83–85.

Keats JJ, Chesi M, Egan JB, Egan JB, Garbitt VM, Palmer SE, Braggio E, Van Wier S, Blackburn PR, Baker AS,

Dispenzieri A, Kumar S, Rajkumar SV, Carpten JD, Barrett M, Fonseca R, Stewart AK, Bergsagel PL. 2012. Clonal competition with alternating dominance in multiple myeloma. Blood 120(5):1067–1076.

Keats JJ, Maxwell CA, Taylor BJ, Hendzel MJ, Chesi M, Bergsagel PL, Larratt LM, Mant MJ, Reiman T, Belch AR, Pilarski LM. 2005. Overexpression of transcripts originating from the MMSET locus characterizes all t(4;14)(p16;q32)-positive multiple myeloma patients. Blood 105(10):4060–4069.

Keats JJ, Reiman T, Maxwell CA, Taylor BJ, Larratt LM, Mant MJ, Belch AR, Pilarski LM. 2003. In multiple myeloma, t(4;14)(p16;q32) is an adverse prognostic factor irrespective of FGFR3 expression. Blood 101(4):1520–1529.

Kim DJ, Li Y, Reddy K, Lee MH, Kim MO, Cho YY, Lee SY, Kim JE, Bode AM, Dong Z. 2012. Novel TOPK inhibitor HI-TOPK-032 effectively suppresses colon cancer growth. Cancer Res 72(12):3060–3068.

Kishimoto T. 2010. IL-6: from its discovery to clinical applications. Int Immunol 22(5):347–352.

Kuiper R, Broyl A, de Knegt Y, van Vliet MH, van Beers EH, van der Holt B, el Jarari L, Mulligan G, Gregory W, Morgan G, Goldschmidt H, Lokhorst HM, van Duin M, Sonneveld P. 2012. A gene expression signature for high-risk multiple myeloma. Leukemia 26(11):2406–2413.

Kumar SK, Rajkumar V, Kyle RA, van Duin M, Sonneveld P, Mateos MV, Gay F, Anderson KC. 2017. Multiple myeloma. Nat Rev Dis Primers 3:17046.

Kwon CH, Park HJ, Choi YR, Kim A, Kim HW, Choi JH, Hwang CS, Lee SJ, Choi CI, Jeon TY, Kim DH, Kim GH, Park do Y. 2016. PSMB8 and PBK as potential gastric cancer subtype-specific biomarkers associated with prognosis. Oncotarget 7(16):21454–21468.

Lim CP, Cao X. 2001. Regulation of Stat3 activation by MEK kinase 1. J Biol Chem 276(24):21004–21011.

Lin A, Giuliano CJ, Palladino A, John KM, Abramowicz C, Yuan ML, Sausville EL, Lukow DA, Liu L, Chait AR, Galluzzo ZC, Tucker C, Sheltzer JM. 2019. Off-target toxicity is a common mechanism of action of cancer drugs undergoing clinical trials. Sci Transl Med 11(509): eaaw8412.

Matsumoto S, Abe Y, Fujibuchi T, Takeuchi T, Kito K, Ueda N, Shigemoto K, Gyo K. 2004. Characterization of a MAPKK-like protein kinase TOPK. Biochem Biophys Res Commun 325(3):997–1004.

Matsuo Y, Park JH, Miyamoto T, Yamamoto S, Hisada S, Alachkar H, Nakamura Y. 2014. TOPK inhibitor induces complete tumor regression in xenograft models of human cancer through inhibition of cytokinesis. Sci Transl Med 6(259):259ra145.

Mikhael JR, Dingli D, Roy V, Reeder CB, Buadi FK, Hayman SR, Dispenzieri A, Fonseca R, Sher T, Kyle RA, Lin Y, Russell SJ, Kumar S, Bergsagel PL, Zeldenrust SR, Leung N, Drake MT, Kapoor P, Ansell SM, Witzig TE, Lust JA, Dalton RJ, Gertz MA, Stewart AK, Rajkumar SV, Chanan-Khan A, Lacy MQ; Mayo Clinic. 2013. Management of newly diagnosed symptomatic multiple myeloma: updated Mayo Stratification of Myeloma and Risk-Adapted Therapy (mSMART) consensus guidelines 2013. Mayo Clin Proc 88(7):360–376.

Moreau P, San Miguel J, Sonneveld P, Mateos MV, Zamagni E, Avet-Loiseau H, Hajek R, Dimopoulos MA, Ludwig H, Einsele H, Zweegman S, Facon T, Cavo M, Terpos E, Goldschmidt H, Attal M, Buske C; ESMO Guidelines Committee. 2017. Multiple myeloma: ESMO Clinical Practice Guidelines for diagnosis, treatment and follow-up. Ann Oncol 28(Suppl. 4):iv52–iv61.

Nagoshi H, Taki T, Hanamura I, Nitta M, Otsuki T, Nishida K, Okuda K, Sakamoto N, Kobayashi S, Yamamoto-Sugitani M, Tsutsumi Y, Kobayashi T, Matsumoto Y, Horiike S, Kuroda J, Taniwaki M. 2012. Frequent PVT1 rearrangement and novel chimeric genes PVT1-NBEA and PVT1-WWOX occur in multiple myeloma with 8q24 abnormality. Cancer Res 72(19):4954–4962.

Ohashi T, Komatsu S, Ichikawa D, Miyamae M, Okajima W, Imamura T, Kiuchi J, Kosuga T, Konishi H, Shiozaki A, Fujiwara H, Okamoto K, Tsuda H, Otsuji E. 2017. Overexpression of PBK/TOPK relates to tumour malignant potential and poor outcome of gastric carcinoma. Br J Cancer 116(2):218–226.

Ohashi T, Komatsu S, Ichikawa D, Miyamae M, Okajima W, Imamura T, Kiuchi J, Nishibeppu K, Kosuga T, Konishi H, Shiozaki A, Fujiwara H, Okamoto K, Tsuda H, Otsuji E. 2016. Overexpression of PBK/TOPK contributes to tumor development and poor outcome of esophageal squamous cell carcinoma. Anticancer Res 36(12):6457–6466.

Ota A, Nakao H, Sawada Y, Karnan S, Wahiduzzaman M, Inoue T, Kobayashi Y, Yamamoto T, Ishii N, Ohashi T, Nakade Y, Sato K, Itoh K, Konishi H, Hosokawa Y, Yoneda M. 2017. Δ40p53α suppresses tumor cell proliferation and induces cellular senescence in hepatocellular carcinoma cells. J Cell Sci 130(3):614–625.

Ozaki S, Wolfenbarger D, deBram-Hart M, Kanangat S, Weiss DT, Solomon A. 1994. Characterization of a novel interleukin-6 autocrine-dependent human plasma cell line. Leukemia 8(12):2207–2213.

Park JH, Nishidate T, Nakamura Y, Katagiri T. 2010. Critical roles of T-LAK cell-originated protein kinase in cytokinesis. Cancer Sci 101(2):403–411.

Quan C, Xiao J, Duan Q, Yuan P, Xue P, Lu H, Yan M, Guo D, Xu S, Zhang X, Lin X, Wang Y, Dogan S, Zhang J, Zhu F, Ke C, Liu L. 2017. T-lymphokine-activated killer cell-originated protein kinase (TOPK) as a prognostic factor and a potential therapeutic target in glioma. Oncotarget 9(8):7782–7795.

Ran FA, Hsu PD, Wright J, Agarwala V, Scott DA, Zhang F. 2013. Genome engineering using the CRISPR-Cas9 system. Nat Protoc 8(11):2281–2308.

Sanjana NE, Shalem O, Zhang F. 2014. Improved vectors and genome-wide libraries for CRISPR screening. Nat Methods 11(8):783–784.

Santra M, Zhan F, Tian E, Barlogie B, Shaughnessy J, Jr. 2003. A subset of multiple myeloma harboring the t(4;14)(p16;q32) translocation lacks FGFR3 expression but maintains an IGH/MMSET fusion transcript. Blood 101(6):2374–2376.

Shah V, Sherborne AL, Walker BA, Johnson DC, Boyle EM, Ellis S, Begum DB, Proszek PZ, Jones JR, Pawlyn C, Savola S, Jenner MW, Drayson MT, Owen RG, Houlston RS, Cairns DA, Gregory WM, Cook G, Davies FE, Jackson GH, Morgan GJ, Kaiser MF. 2018. Prediction of outcome in newly diagnosed myeloma: a meta-analysis of the molecular profiles of 1905 trial patients. Leukemia 32(1):102–110.

Stewart SA, Dykxhoorn DM, Palliser D, Palliser D, Mizuno H, Yu EY, An DS, Sabatini DM, Chen IS, Hahn WC, Sharp PA, Weinberg RA, Novina CD. 2003. Lentivirus-delivered stable gene silencing by RNAi in primary cells. RNA 9(4):493–501.

Takahashi M, Ota A, Karnan S, Hossain E, Konishi Y, Damdindorj L, Konishi H, Yokochi T, Nitta M, Hosokawa Y.

2013. Arsenic trioxide prevents nitric oxide production in lipopolysaccharide -stimulated RAW 264.7 by inhibiting a TRIF-dependent pathway. Cancer Sci 104(2):165–170.

Takeda K, Noguchi K, Shi W Tanaka T, Matsumoto M, Yoshida N, Kishimoto T, Akira S. 1997. Targeted disruption of the mouse Stat3 gene leads to early embryonic lethality. Proc Natl Acad Sci U S A 94(8):3801–3804.

Wahiduzzaman M, Ota A, Karnan S, Hanamura I, Mizuno S, Kanasugi J, Rahman ML, Hyodo T, Konishi H, Tsuzuki S, Takami A, Hosokawa Y. 2018. Novel combined Ato-C treatment synergistically suppresses proliferation of Bcr-Abl-positive leukemic cells in vitro and in vivo. Cancer Lett 433: 117–130.

Yang YF, Pan YH, Cao Y, Fu J, Yang X, Zhang MF, Tian QH. 2017. PDZ binding kinase, regulated by FoxM1, enhances malignant phenotype via activation of β-Catenin signaling in hepatocellular carcinoma. Oncotarget 8(29):47195–47205.

Address correspondence to:
Dr. Akinobu Ota
Department of Biochemistry
Aichi Medical University School of Medicine
1-1 Yazakokarimata, Building No. 2, Room 362
Nagakute 480-1195
Aichi
Japan

E-mail: aota@aichi-med-u.ac.jp

Received 25 May 2020/Accepted 14 June 2020